Physics Letters A 374 (2010) 4090–4098

Contents lists available at ScienceDirect

Physics Letters A

www.elsevier.com/locate/pla

Decoherence and classical behavior with a chaotic macroscopic environment

Nikola Burić

Institute of Physics, University of Belgrade, PO BOX 68, 11000 Belgrade, Serbia

ARTICLE INFO

Article history:
Received 23 February 2010
Received in revised form 14 April 2010
Accepted 4 May 2010
Available online 7 May 2010
Communicated by P.R. Holland

ABSTRACT

Quantum state diffusion approach to open system dynamics is used to study decoherence and dynamics of the pointer observable of an angular momentum system in interaction with a macroscopic nonlinear and dissipative environment. It is shown that dispersion of the pointer observable in the mixed state of the open system is clearly larger if the environment is classically chaotic then in the case of the environment with regular dynamics.

1. Introduction

Possibility of classical behavior of objects described by quantum mechanics is the major contribution of the theory of decoherence to the understanding of quantum mechanics [1–3]. Interaction, and the consequent entanglement, between the considered quantum system S and an another system with large number of degrees of freedom, called environment and denoted E, implies that some of the system's S observables, called pointer variables, behave as classical physical quantities. The only dynamically stable states of S are such that the chosen observable, i.e. the pointer variable, most of the time during the evolution possess sharp values with negligible dispersion. This is considered as a necessary property for the classical behavior of the pointer variable.

Standard models that have been used to demonstrate and study the decoherence are based on environments with trivial dynamics [1]. It is supposed that the environment has the large number of degrees of freedom so that the recurrence times can be assumed to be arbitrary long. Furthermore, some sort of dissipation of information or coarse graining is performed so that the precise quantum (micro-state) of the environment is not known. However, nontrivial dynamical properties of the environment might have crucial influence on the decoherence process and on the dynamical stability of the pointer variable. For example, since the environment is assumed to behave essentially like a macroscopic system it is justified to study the decoherence due to environments that can display classically chaotic behavior. It is the purpose of this work to explore the decoherence and the behavior of the pointer variable in a system coupled to an environment that can display dynamics with properties typical of classical nonlinear dissipative systems, like the chaotic behavior.

The importance of the environment dynamics is appreciated but is not well understood, which is the reason for relatively recent interest in the decoherence due to the environments with interesting dynamics. Decoherence by environments that have nontrivial quantum dynamics, for example by kicked tops [4], kicked rotators [5,6], spin chains [7–9] or abstract models [10–12], has been studied. Such studies lead to somewhat controversial and incomplete conclusions. Our work is in the same general spirit of these studies, of exploring decoherence with dynamically interesting environments, but is essentially different because we shall use for the environment a system which in the macroscopic limit has properties of chaotic systems in the well-defined sense of classical dynamical systems. As is well known, the dynamics of a quantum system with finite number of degrees of freedom is always integrable, i.e. the states follow either periodic or quasi-periodic orbits. Thus, the environment must itself behave approximately as a classical system in order to approximately displays the dynamical chaos. Complexity of the dynamics of the quantum systems that are used in the quoted references to play the role of the environment, is identified with certain properties of their spectral distributions or with the chaoticity of the corresponding classical model. Neither of these is equivalent to the existence of chaotic state evolution. These properties also do not imply chaoticity of the approximate phase space trajectories, i.e. these properties do not imply existence of the phase space localized wave packet whose centroid approximately displays classically chaotic evolution for all times. The correspondence of the evolution of the quantum wave packets with the classical chaotic dynamics is valid only up to the Ehrenfest time. On the contrary, the system that we shall use to model the environment is an open quantum system that in the macroscopic limit can display the dynamical chaos and the bifurcations typical of a nonlinear dissipative classical systems. We have used the same model of the environment to study the influence of such environments on the entanglement between two qubits [13]. The same environment was recently used also to model the process of measurement performed on a single qubit [14]. In this Letter we concentrate on the dynamical behavior of the pointer observable of a quantum system of variable size coupled to such

E-mail address: buric@phy.bg.ac.yu.

0375-9601/$ – see front matter © 2010 Published by Elsevier B.V.
doi:10.1016/j.physleta.2010.05.009

macroscopic environment with different dynamical properties. Our study clearly shows the implications of different classical dynamical properties of the macroscopic environment on the decoherence and dynamics of the pointer observable. Furthermore it is demonstrated that application of quantum trajectories approach to the open system dynamics is crucial in obtaining the proper understanding of these differences.

The Letter is organized as follows. In Section 2 the model to be studied is introduced, and we briefly recapitulate the quantum state diffusion (QSD) [15] approach to the open quantum system dynamics which is the main tool of our analyzes. In Section 3 we present the results of our numerical computations and our main conclusions concerning the decoherence by regular or chaotic macroscopic environment. In Section 4 a classical model of the quantum system given by equations on the classical phase space is analyzed. Section 5 presents a summary and discussion of our results.

2. The system and the environment

We shall study the system that is composed of a quantum subsystem and its macroscopic environment. Dynamics of the quantum subsystem, when isolated from the environment, is described by the following Hamiltonian

$$H = -2\alpha J_x + 2\epsilon J_z + c J_z^2, \tag{1}$$

where J_x, J_y, J_z satisfy $SU(2)$ commutation relations, with $\hbar = 1$. Thus, $SU(2)$ is the dynamical group of the system (1). The $SU(2)$ symmetry also suggests a special set of initial states, that is the $SU(2)$ coherent states [16,17]. However, notice that the Hamiltonian is a nonlinear expression of the group generators, so that the set of $SU(2)$ coherent states is not invariant on the evolution of the system (1). Consequently evolution of the averages $\langle J_{x,y,z}\rangle$ generated by (1) does not satisfy the equations of the classical mean field approximation. The classical limit corresponds to large value of the Casimir operator J^2. If the nonlinearity parameter $c \ll J^2$ the dynamics of (1) is well approximated by the mean-field equations in the $SU(2)$ coherent states. We shall be interested only in the situation when the parameter $\alpha = const$. In this case the dynamics of the averages over an initial coherent state of $\langle J_{x,y,z}\rangle$ represents regular periodic oscillations.

Physically the Hamiltonian (1) can be realized as a two mode Bose–Hubbard system, given by

$$H = \epsilon_1 a_1^\dagger a_1 + \epsilon_2 a_2^\dagger a_2 + \alpha\left(a_1^\dagger a_2 + a_2^\dagger a_1\right) + c\left(a_1^{\dagger 2} a_1^2 + a_2^{\dagger 2} a_2^2\right), \tag{2}$$

where $\epsilon = \epsilon_1 - \epsilon_2$ and a_i, $a_i^\dagger$, $i = 1, 2$ are bosonic operators [17]. The correspondence between (1) and (2) is established by expressing the angular momentum operators J_x, J_y, J_z in terms of a_i, $a_i^\dagger$ as follows

$$J_x = \frac{1}{2}\left(a_1^\dagger a_2 + a_2^\dagger a_1\right),$$
$$J_y = \frac{i}{2}\left(a_1^\dagger a_2 - a_2^\dagger a_1\right),$$
$$J_z = \frac{1}{2}\left(a_2^\dagger a_2 - a_1^\dagger a_1\right). \tag{3}$$

The total particle number $N = n_1 + n_2$ is related to the $J^2 = N(N/2 + 1)/2$ and is conserved. Large values of J correspond to large total number of quanta.

We would like to couple the quantum system (1) to an environment that can behave as a classical dissipative nonlinear system. As a formal model of such an environment we shall use an inverted oscillator with quartic nonlinearity and dissipation. Furthermore we shall suppose that the environment satisfies the Markov assumption. The system representing the environment is characterized by its Hamiltonian H_e and the Lindblad L operators given by [18]

$$H_e = P^2/2 + \beta^2 Q^4/4 - Q^2/2 + g\cos(t)Q/\beta + \gamma(QP + PQ)/2, \tag{4}$$

$$L = \sqrt{2\gamma}a = \sqrt{2\gamma}(Q - iP)/\sqrt{2}. \tag{5}$$

In the dynamical system theory chaoticity of dynamics is defined in terms of orbits of an individual system, i.e. by orbits through points in the system's phase space. The description of the dynamics in terms of the evolution of an ensemble of systems i.e. in terms of probability densities on the phase space is of course equivalent but the chaoticity of an individual system orbit is made less obvious in the averaged description by the probability densities. Our goal is to explore the influence of an environment whose dynamical behavior is that of a typical classically chaotic system. In order to capture this chaotic dynamics it is preferable to use the description of the quantum dynamics in terms of evolution of individual systems, and not that of ensembles. Complete description of a state of an open quantum system is given by its density matrix ρ, and the evolution is commonly described by the corresponding master equation for $\rho(t)$ [19]. The evolution equation is linear and the description corresponds to an ensemble of quantum systems, analogously to the Liouvile or Focker–Planck evolution equations for the probability densities of classical ensembles. On the other hand, the mixed state is equivalent to a random pure state, and the evolution of the pure state vector of a single open quantum system can often be described by the Schroedinger equation with additional terms due to dissipation and stochastic fluctuations [20,21,15,19]. Stochastic Schroedinger equations (SSE) are obtained by unraveling the master equation for $\rho(t)$ and they are all consistent with the requirement that the solutions of the master equation and of the SSE satisfy

$$\rho(t) = E\left[\left|\psi(t)\right\rangle\left\langle\psi(t)\right|\right], \tag{6}$$

where $E[|\psi(t)\rangle\langle\psi(t)|]$ is the expectation with respect to the distribution of the random vector $|\psi(t)\rangle$.

In the case of continuous Markov evolution the unique SSE for the stochastic state vector $|\psi(t)\rangle$ which has the same symmetry properties as the Markov master equation in the Lindblad form for $\rho(t)$ [22,23,19], represent a complex diffusion process on the open system's Hilbert space and is given by the theory of quantum state diffusion (QSD) [15]. The QSD evolution equation reads

$$|d\psi\rangle = -iH|\psi\rangle\,dt + \left[\sum_k 2\left\langle L_k^\dagger\right\rangle L_k - L_k^\dagger L_k - \left\langle L_k^\dagger\right\rangle\langle L_k\rangle\right]\left|\psi(t)\right\rangle dt + \sum_k\left(L_k - \langle L_k\rangle\right)\left|\psi(t)\right\rangle dW_k \tag{7}$$

where $\langle\rangle$ denotes the quantum expectation in the state $|\psi(t)\rangle$ and dW_k are independent increments of complex Wiener c-number processes $W_k(t)$ satisfying

$$E[dW_k] = E[dW_k\,dW_{k'}] = 0, \qquad E[dW_k\,d\bar{W}_{k'}] = \delta_{k,k'}\,dt, \quad k = 1, 2, \ldots, m. \tag{8}$$

Here $E[\cdot]$ denotes the expectation with respect to the probability distribution given by the multi-dimensional process W, and $\bar{W}_k$ is the complex conjugate of W_k.

There are two main approaches to the unraveling of the Lindblad master equation: the method of quantum state diffusion [15] and the relative state method [21,19], with specific advantages associated with each of the methods. The relative state method is usually used do describe the situations when the measurement is the dominant interaction with the environment. The method offers particular flexibility in that the master equation can be unraveled into different stochastic equations conditioned on the results of measurement. On the other hand the correspondence between the QSD equations and the Linblad master equations is unique, and is not related to a particular measurement scheme, or the form of the Markov environment.

QSD approach has been used often to study decoherence and the classical limit [18,24–27,14,28–30,13,31]. In principle there is an infinity of possible unravellings of the master equation consistent with (6), and some, like quantum jumps [21,19] or real diffusion [19] models are commonly used. However, the classical limit of different unravellings of the Lindblad master equation has been shown to result in the same dynamical picture [32]. Thus, for our purpose of representing the effects of environment in the classical limit, all unravellings should produce approximately the same single system dynamics as the unraveling given by the QSD which we shall use.

The dynamics of the environment (4) and (5) crucially depends on the parameters β and g and to the lesser extent on γ. The parameter β characterizes the classicality of the system in the sense that the classical i.e. macroscopic limit is realized by rescaling $\beta \to 0$, which leads to the large ratio of the phase space covered by the system's motion and the area of the Planks cell. Also appropriate values of γ imply good localization in the sense that the dispersion of the dynamical variables is negligible with respect to their variations during the motion. If β is sufficiently small and for appropriate γ the QSD equation (7) with (4) and (5) reproduces the qualitative and quantitative properties of the classical Duffing oscillator, described by

$$\frac{d^2q}{dt^2} + 2\gamma\frac{dq}{dt} + q^3 - q = g\cos(t). \tag{9}$$

Depending on the parameter g the classical system (9) can have simple regular attractors like fixed points or periodic orbits, or a complicated chaotic attractor [33]. The open quantum system, given by (4) and (5), which is considered here as the environment of the system (1), for sufficiently small β, reproduces the classical dynamics of the Duffing oscillator. For example, for $g = 0.3$, $\gamma = 0.125$ and for small β, say $\beta = 0.01$ the averages $\langle Q(t)\rangle$, $\langle P(t)\rangle$ of the open system (4) and (5) reproduce the chaotic trajectories of the classical Duffing oscillator [18]. This represents our model of the nonlinear classically chaotic environment.

The coupling between the quantum system (1) and its environment (4) and (5) is given by

$$H_{int} = \mu J_z Q. \tag{10}$$

The environment is coupled to J_z so it is expected that J_z has classical properties, i.e. the dispersion $\Delta_{\psi(t)} J_z = \langle\psi(t)|J_z^2|\psi(t)\rangle - \langle\psi(t)|J_z|\psi(t)\rangle^2$ should quickly become and remain small. We shall also briefly discuss other types of coupling.

In summary, we have a model that consists of a quantum system (1) with the nonlinear Hamiltonian and of variable size (parameter J) which interacts with the environment, given by (4) and (5), that can behave as a classical system (for β small) and in such regime can display classically regular or chaotic dynamics (parameter g).

3. Numerical results

In this section we present results of numerical computations that are aimed at getting an understanding of the role of various parameters that influence behavior of the dispersions

$$\Delta_{\psi(t)} A = \langle\psi(t)|A^2|\psi(t)\rangle - \langle\psi(t)|A|\psi(t)\rangle^2 \tag{11}$$

and

$$\Delta_{\rho(t)} A = Tr[\rho A^2] - Tr[\rho A]^2 \tag{12}$$

of an observable A in the random pure state $\psi(t)$ (11) or the mixed state $\rho(t) = E(|\psi\rangle\langle\psi|)$ (12). The total system is an open system and thus its state is represented by the corresponding density matrix or by an ensemble of pure states, i.e. by random pure states. The dispersion (11) represents purely quantum part of the total dispersion in the mixed state $\rho = E(|\psi\rangle\langle\psi|)$ [19,34,35,31]. The pure state dispersion measures the distance of the random pure state $|\psi(t)\rangle$ from an eigenstate of the operator A, and its ensemble average represent the average dispersion in pure states that appear in the resolution of ρ. Thus, it is a measure of average intrinsic quantum variance. Total dispersion (12) in the mixed state $\rho(t)$ is different from the ensemble average of the pure state dispersions (11). The total dispersion $\Delta_{\rho(t)} A$ contains an additional term which represents the dispersion of the c-number $\langle\psi|A|\psi\rangle$ and represent statistical fluctuation of this classical quantity. We shall use both types of dispersions $\Delta_{\psi(t)}$ and $\Delta_{\rho(t)}$ to study the appearance of classical behavior, and compare the information that can be obtained from one or the other.

All results that shall be presented were computed with rather small value of β since we wanted the environment to behave as a macroscopic system, and its dynamics to be qualitatively sensitive to the values of the bifurcation parameter g. Our main interest is in the dependence of the dispersion (11) on the values of g that correspond to regular behavior, like stationary or periodic states, or to the chaotic dynamics. On the way we shall observe also the dependence of (11) on the influence of the size of the quantum subsystem, i.e. the size of J, and on the type of the subsystem environment coupling. All numerical results that we use here to illustrate the effects of decoherence were obtained with initial states in the form of $SU(2)$ coherent states

$$|\theta,\psi\rangle = \frac{1}{\sqrt{N!}}\left(\cos(\theta/2)a_1^\dagger + \sin(\theta/2)\exp(-i\phi)a_2^\dagger\right)^N|0,0\rangle \tag{13}$$

with different J, but other initial states lead to qualitatively the same conclusions. All our computations were performed with the same values of $\omega = 1$, $\alpha = 1$, $\epsilon = 0$, $c = 0.25$, $\gamma = 0.125$, and various time series are always presented in terms of the dimensionless time $t \equiv \omega t$.

3.1. Main results

Fig. 1 illustrates the effects of decoherence and the influence of different coupling strength on $\langle J_z\rangle$ and $\Delta_\psi J_z$ when the environment exhibits the regular motion in the form of convergence to the stationary state. The values of the coupling parameter are $\mu = 0$; 0.1; 0.5 and $J = 6$. The conclusion is expected and obvious: stronger interaction with the environment imply faster convergence of J_z to one of its eigenstates.

In Figs. 2(a)–(f) illustrated are $\langle J_z\rangle$ and $\Delta_\psi J_z$ for different dynamical behavior of the environment, characterized by $g = 0.001$ (fixed point attractor) $g = 0.15$ (limit cycle attractor) and $g = 0.3$ (chaotic attractor), for three values of μ and for $J = 6$. It is clear that the regular dynamics of the environment, i.e. the stationary state and the periodic oscillations, imply similar behavior of $\langle J_z\rangle$ and $\Delta_\psi J_z$. In both situations $|\psi\rangle$ approaches an eigenstate of J_z and remains near the eigenstate. On the other hand, chaotic dynamics of the environment leads to faster approach to an eigenstate, but then $|\psi\rangle$ moves fast through the states with large $\Delta_\psi J_z$. This cycle is irregularly repeated forever. $\Delta_\psi J_z$ does not remain near $\Delta_\psi J_z = 0$, like it does with the regular environment. We shall

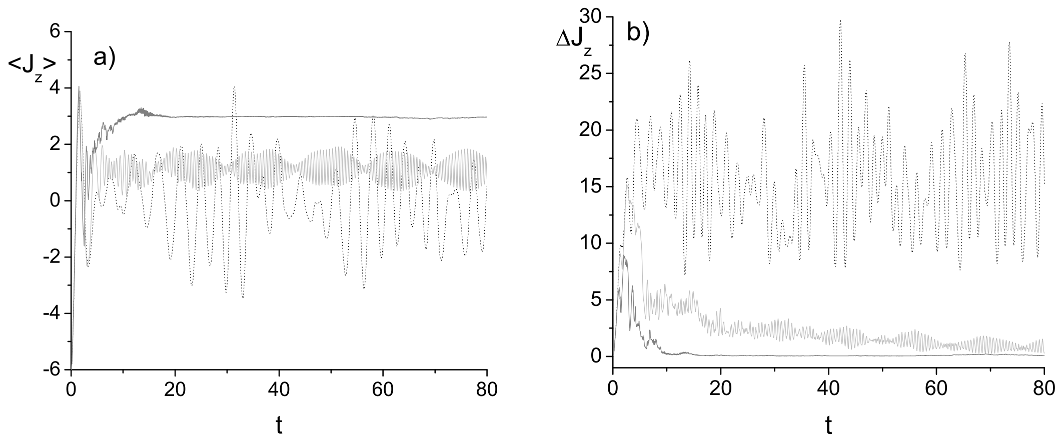

Fig. 1. Illustrates dynamics of the pointer observable $\langle J_z(t)\rangle$ (a) and its dispersion $\Delta_{|\psi(t)\rangle} J_z \equiv \Delta J_z$ (b) for the regular environment $g = 0.001$ and $\mu = 0$ (gray dotted); $\mu = 0.1$ (light gray full); and $\mu = 0.5$ (black full). Other parameters are $J = 6$, $\beta = 0.01$.

see that such behavior of $\langle J_z\rangle$ is qualitatively reproduced by a classical model of the quantum system. Thus, although $\Delta_\psi J_z$ is not small all the time, like it is in the case of the regular environments, the behavior of $\langle J_z\rangle$ can be considered as classical as far as its dispersion $\Delta_\psi J_z$ is considered.

In Fig. 3 we compare the dynamics of $\langle J_z\rangle$ with the dynamics of environmental variable $\langle Q\rangle$. Periods during which $\Delta_\psi J_z$ is large correspond to large variations of $\langle Q\rangle$ that occur during the chaotic motion of the environment. There are no such large variations when the dynamics of the environment is regular, either stationary or oscillatory, and thus $|\psi\rangle$ remains close to an eigenstate of J_z.

Fig. 4 illustrate the dynamics of $\langle J_y\rangle$ and $\Delta_\psi J_y$ for the coupling $\mu = 0.5$ and for different types of the environment. As expected it is obvious that the variable $\langle J_y\rangle$ (and similarly $\langle J_x\rangle$, not shown) has large dispersions all the time and cannot be considered as classical, with no important qualitative dependence on the environment.

Fig. 5 illustrates dependence of decoherence and the dynamics of $\Delta_\psi J_z$ on the size of J. Larger J implies faster decoherence, i.e. faster approach of $\Delta_\psi J_z$ to zero, but also larger variations of $\Delta_\psi J_z$. Large variations of $\Delta_\psi J_z$ away from zero due to the chaotic environment occur for any J. For larger J, such a large variation is followed by fast decoherence $\Delta_\psi J_z \to 0$, new large variation and so on. Permanently occurring large variations of $\Delta_\psi J_z$ do not happen if the dynamics of the environment is regular for any value of J. For any J, decoherence from a large value of $\Delta_\psi J_z$ to $\Delta_\psi J_z \approx 0$ is slower with regular environmental dynamics, and for smaller J, but once the state has approached an eigenstate of J_z it remains there forever.

All the results presented so far are concerned with the behavior of $\langle J_z\rangle$ and $\Delta_\psi J_z$ for a single representative of the ensemble that form the evolving mixed state of the system in the QSD unraveling. In order to compute the total dispersion (12) in this mixed state $\Delta_\rho J_z$ we need first to compute $\rho(t) = E(|\psi(t)\rangle\langle\psi(t)|)$ and then the required averages of J_z and J_z^2, which is different from the ensemble average $E(\Delta_\psi J_z)$. $Tr[\rho J_z]$ and the total dispersion $\Delta_\rho J_z$ are illustrated in Fig. 6 and compared with the corresponding quantities for the typical random state $|\psi(t)\rangle$. Again, the total dispersion $\Delta_\rho J_z$ has similar values for the environments with the two types of regular dynamics but is quite different and significantly larger if the environment is classically chaotic. However, here the dynamical explanation for the large values of the total dispersion in the case of chaotic environment is hidden by the averaging. Large values of total dispersion would indicate the non-classical behavior of J_z, but the picture provided by the unraveling of $\rho(t)$ by the stochastic states $|\psi(t)\rangle$ clearly shows the dynamical origin of the large dispersions. Let us stress again that in our situation of the macroscopic limit, corresponding to small β, different unraveling of the master equation, for example by the quantum jumps approach, would provide essentially the same picture as the QSD approach. Data presented in Fig. 6 were computed with only 200 sample paths, and more sample paths do not qualitatively change the conclusions.

Clear qualitative difference between the effect of the regular vs. chaotic environments can be further illustrated by the time average

$$\overline{\Delta_{\rho(t)}} J_z = \frac{1}{t}\int_0^t \Delta_{\rho(s)}\, ds$$

of the total dispersions presented in Fig. 7.

3.2. Other types of coupling

Type of coupling with the environment determines the observable with small averaged dispersion, and the basis of stable states as opposed to the states that are quickly destroyed. In the previous it was the observable J_z. If J_x (or J_y) appears in (10) instead of J_z than $\langle J_x\rangle$ (or $\langle J_y\rangle$) behaves as approximately classical, and similar properties as those that have been illustrated could be observed. If only one of the operators $J_{x,y,z}$ appears in (10) only that observable has small averaged dispersion and the other two have large dispersions all the time. If all three angular variables are coupled to the same environment, in the form of one Duffing oscillator, i.e. $H_{int} = (J_x + J_y + J_z)Q$, all three angular observables have large dispersions all the time, and none of them can be considered as classical. In this case the observable with small dispersion is given by the sum $A = (J_x + J_y + J_z)$. It would be interesting to study the case when the three angular observables are coupled to three independent Duffing oscillators when one should expect decoherence in all three observables. This system with three independent environments in the form of three Duffing oscillators (4) and (5), which requires considerable numerical resources, will be investigated in the future.

4. Classical model

It is interesting to compare the dynamics of the open quantum system (1) in the environment given by (4) and (5) with dynamics of the corresponding classical model. One expects that the dynamics of the quantum variable that behaves classically in the sense of small dispersion should be at least qualitatively well approximated by the corresponding variable of the classical model.

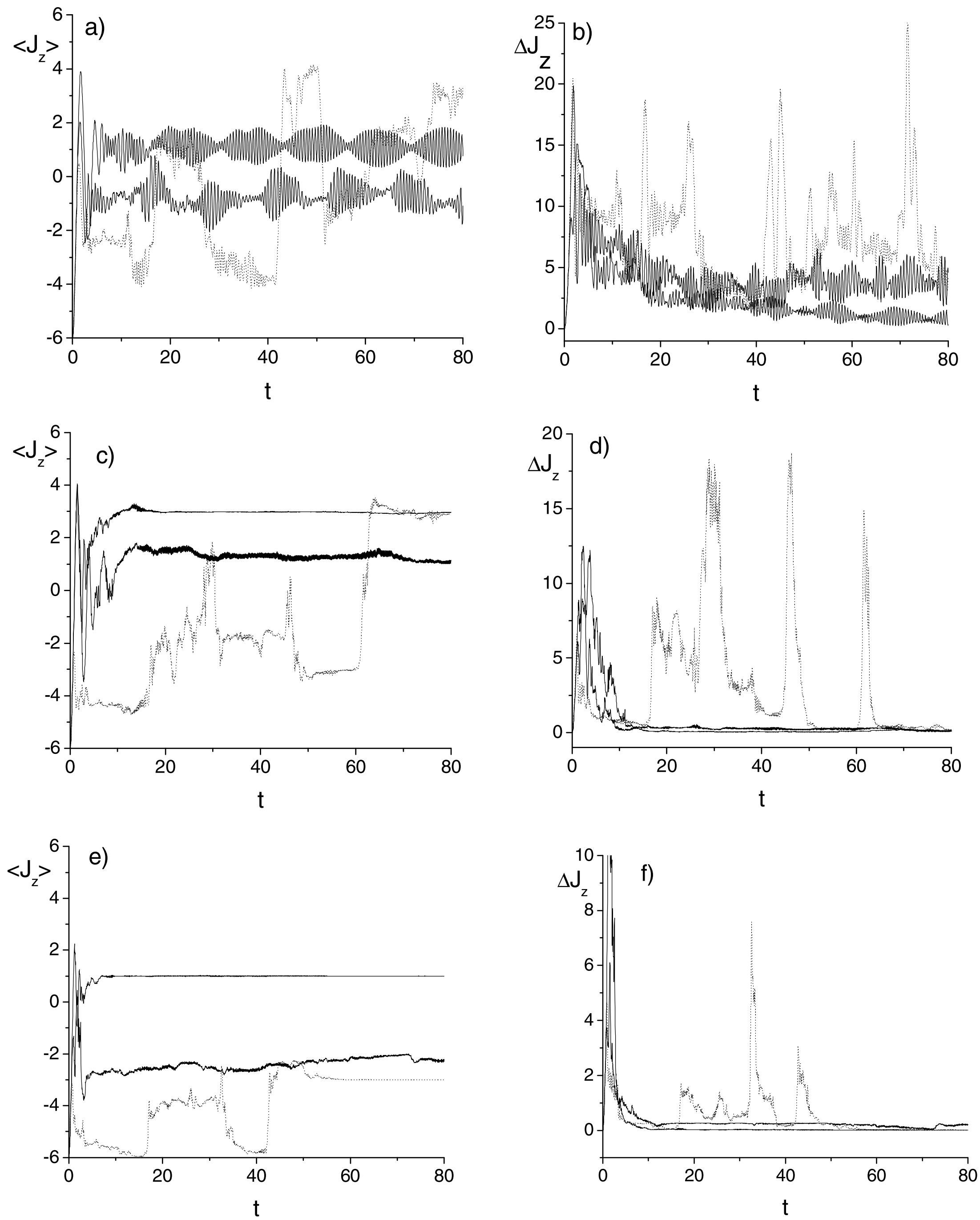

Fig. 2. Illustrates the dependence of $\langle J_z(t)\rangle$ (a, c, e) and $\Delta_{|\psi(t)\rangle} J_z \equiv \Delta J_z$ (b, d, f) on the coupling strength (a) and (b) $\mu = 0.1$; (c) and (d) $\mu = 0.5$; (e) and (f) $\mu = 1$ and on the type of the environment dynamics: $g = 0.001$ (full black) stationary state attractor; $g = 0.15$ (full light gray) limit cycle attractor and $g = 0.3$ (dotted gray) chaotic attractor. Other parameters are $J = 6$, $\beta = 0.01$.

A classical model of the quantum system (1) with the environment (4) and (5) can be obtained by applying the mean field or Ehrenfest approximation on the QSD equations for the averages of the dynamical variables: $\langle J_x\rangle$, $\langle J_y\rangle$, $\langle J_z\rangle$, $\langle Q\rangle$, $\langle P\rangle$. For a general variable $\langle A\rangle$ the dynamical equation corresponding to the QSD evolution equation (7) is of the form

$$d\langle A\rangle = i\langle [H, A]\rangle dt - \frac{1}{2}\langle L^\dagger [L, A] + [A, L^\dagger] L\rangle dt + \sigma(A^\dagger, L)\, dW + \sigma(L, A)\, \overline{dW}, \tag{14}$$

where $\sigma(A, B) = \langle A^\dagger B\rangle - \overline{\langle A\rangle}\langle A\rangle$ and L is the (sum of) Lindblad operator, in our case given by (5).

The approximate equations for $\langle J_x\rangle \equiv j_x$, $\langle J_y\rangle \equiv j_y$, $\langle J_z\rangle \equiv j_z$ are obtained by replacing averages of operator products by products of averaged operators, and are given by

$$\frac{dj_x}{dt} = -2\epsilon j_y - 2c j_z j_y - \mu j_y \langle Q\rangle,$$
$$\frac{dj_y}{dt} = 2\alpha j_z + 2\epsilon j_x + 2c j_x j_z + \mu j_x \langle Q\rangle,$$
$$\frac{dj_z}{dt} = -2\alpha j_y. \tag{15}$$

Because the Lindblad operator commutes with the angular degrees of freedom the drift and the fluctuation parts in Eq. (14) in

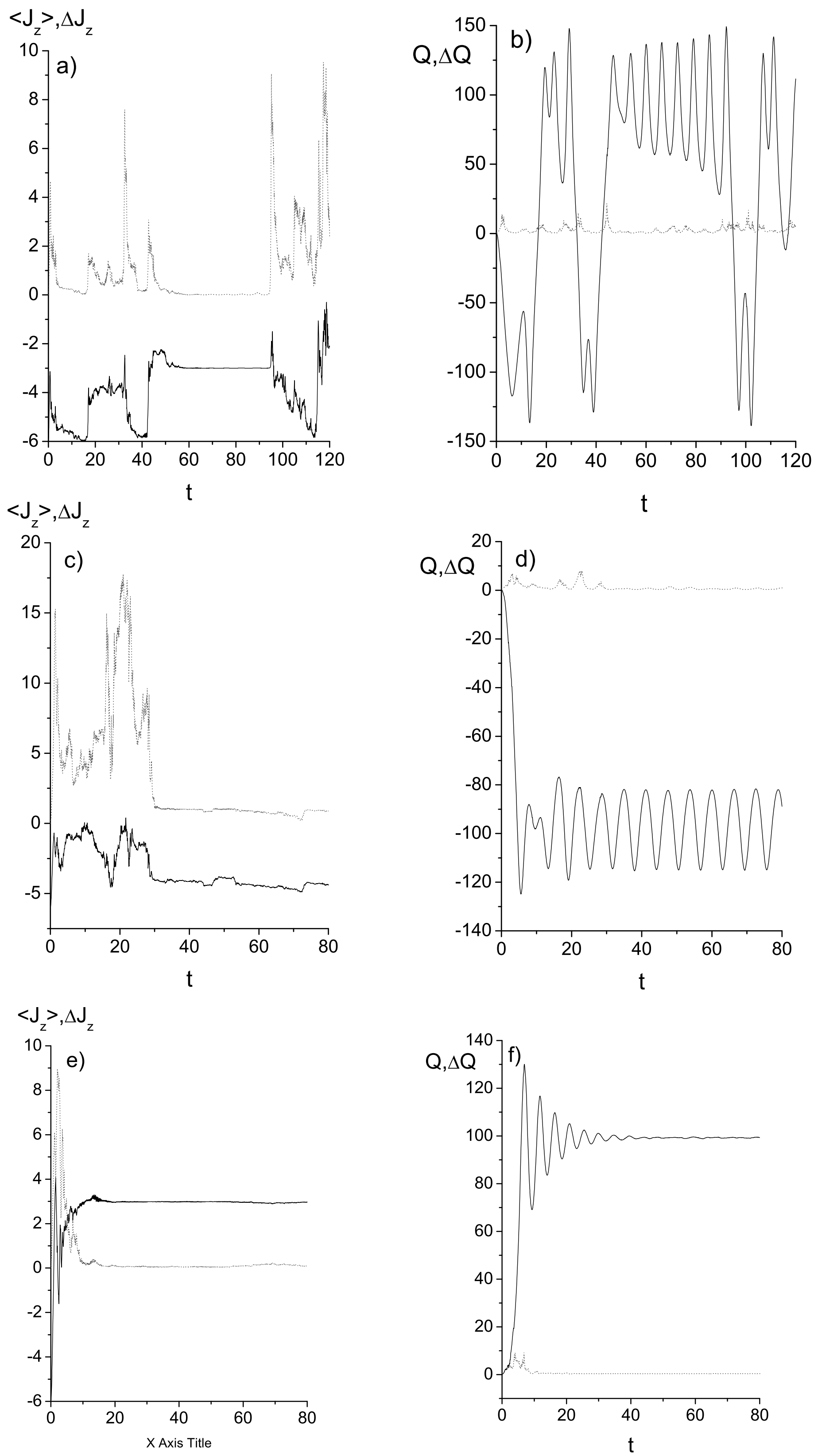

Fig. 3. Comparison of the evolution of $\langle J_z(t)\rangle$ (black full) and $\Delta_{|\psi(t)\rangle} J_z \equiv \Delta J_z$ (gray dotted) (a, c, e) with that of $\langle Q(t)\rangle$ (black full) and $\Delta_{|\psi(t)\rangle} Q \equiv \Delta Q$ (gray dotted) (b, d, f) for the three types of the environment dynamics: (a) and (b) $g = 0.3$ (chaotic); (c) and (d) $g = 0.15$ (limit cycle) and (e) and (f) $g = 0.001$ (stationary state). Other parameters are $J = 6$, $\beta = 0.01$, $\mu = 0.5$.

the case of $\langle J_x\rangle$, $\langle J_y\rangle$, $\langle J_z\rangle$ are zero. The only stochastic terms are generated by $\langle Q\rangle$. It is plausible to further approximate the QSD equations for the variables $\langle Q\rangle$ and $\langle P\rangle$ by the equations of the classical Duffing oscillator, and thus replace the stochastic differential equations by ordinary ones. This approximation is justified in the classical limit of very small β which is the case studied

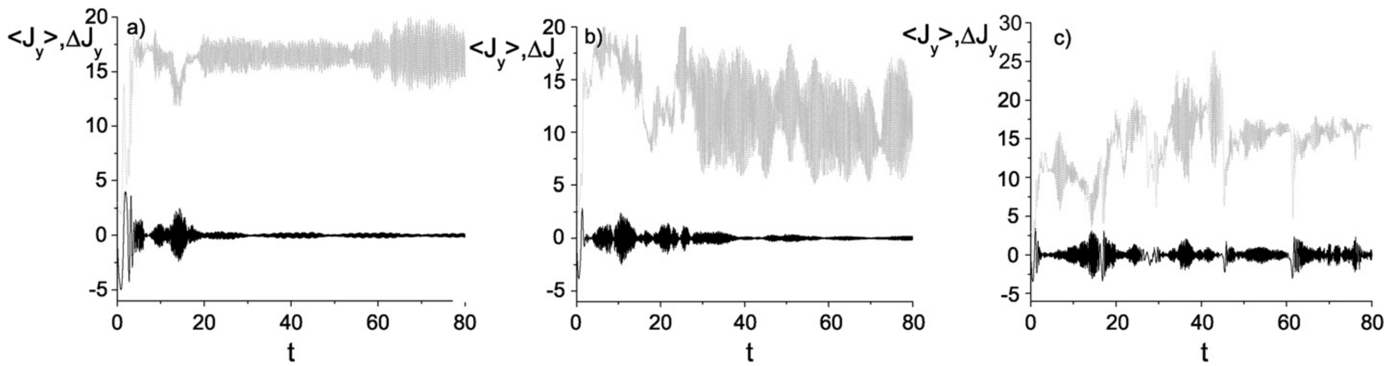

Fig. 4. Illustrates the dependence of $\langle J_y(t)\rangle$ (black) and $\Delta_{|\psi(t)\rangle} J_y \equiv \Delta J_y$ (light gray) on the type of the environment dynamics: $g = 0.001$ (a); $g = 0.15$ (b) and $g = 0.3$ (c). Other parameters are $J = 6$, $\beta = 0.01$.

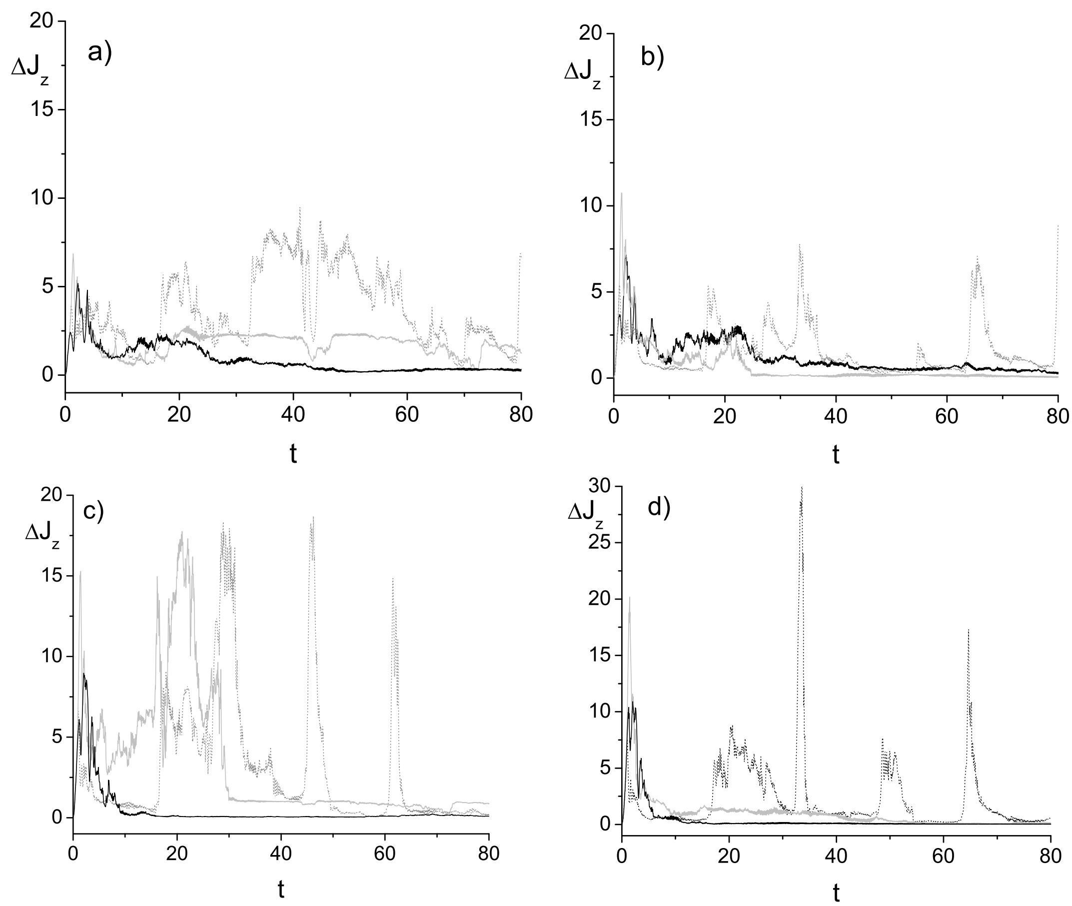

Fig. 5. Illustrates the dependence of $\Delta_{|\psi(t)\rangle} J_z \equiv \Delta J_z$ on the size of the angular momentum: (a) $J = 4$; (b) $J = 5$; (c) $J = 6$ and (d) $J = 7$ for the three types of the environment dynamics: $g = 0.001$ (full black); $g = 0.15$ (full light gray) and $g = 0.3$ (dotted gray). Other parameters are $\mu = 0.5$, $\beta = 0.01$.

here. The Duffing equations with added interaction with $\langle J_z\rangle \equiv j_z$ read

$$dq/dt = p,$$
$$dp/dt = -2\gamma p + \beta^4 q^3 + q - \frac{g}{\beta}\cos(t) - \mu j_z. \qquad (16)$$

Notice that there is no randomness is the evolution of the classical model, given by ordinary differential equations (15) and (16), while the quantum QSD dynamical equation of a single open quantum system explicitly contain stochastic terms.

Eqs. (15) and (16) represent the classical model that we compared with the open quantum system (1) with the environment (4) and (5). The main conclusion of such comparison is that the quantum dynamics of the decohereing variable $\langle J_z\rangle$ is qualitatively well approximated by the dynamics of the classical model. Typical convergence to a fixed values of $\langle J_z\rangle$ in the cases of regular environmental dynamics is well approximated by the dynamics of the classical model, as is illustrated in Figs. 8(a), (b). Chaotic dynamics of the environment induces large end fast variations of the quantum $\langle J_z\rangle$, and this behavior occurs also in the classical model (please see Fig. 8(c)). On the other hand, dynamics of j_x, j_y generated by the classical model is completely different from the corresponding quantum dynamics of $\langle J_x\rangle$, $\langle J_y\rangle$.

5. Summary and discussion

Decoherence and dynamics of the pointer observable under the influence of dynamically different macroscopic environments were

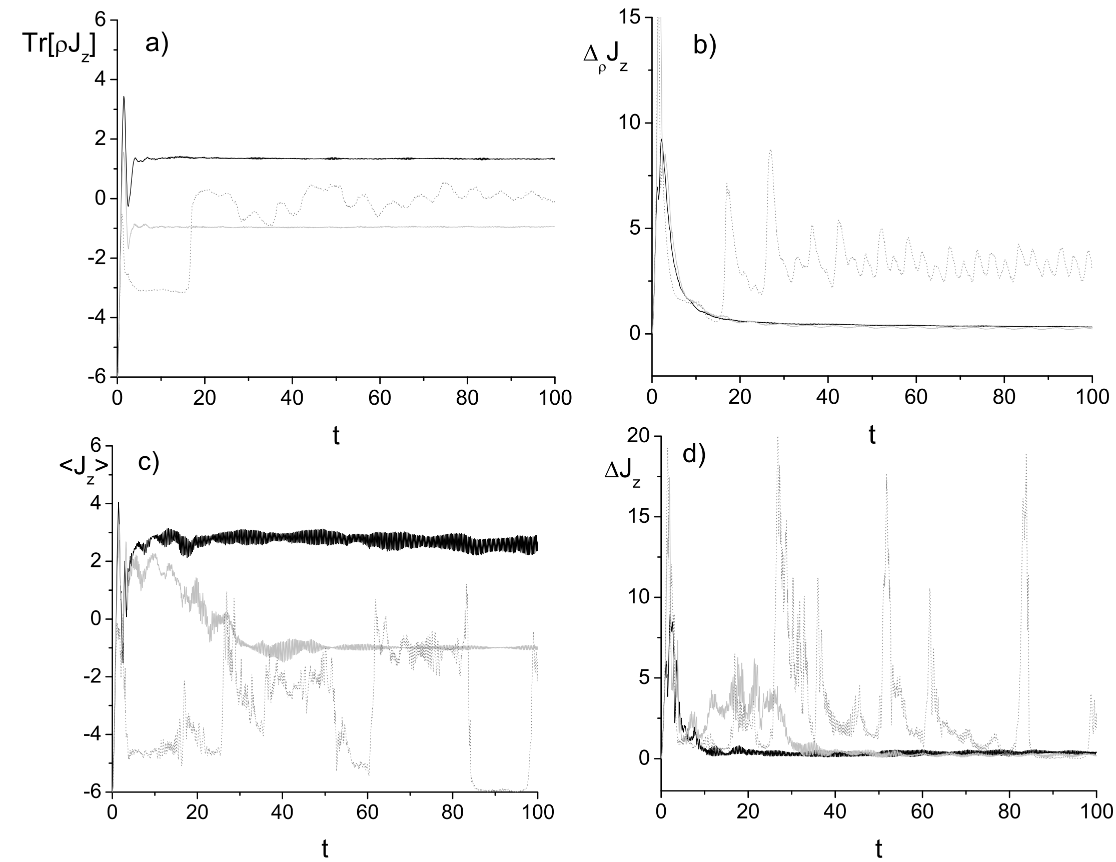

Fig. 6. Illustrated are: mixed state average (a) $Tr[\rho(t)J_z]$; (b) total dispersion $\Delta_{|\rho(t)}J_z$; (c) pure state average $\langle J_z\rangle$ and (d) the pure state dispersion $\Delta_{|\psi(t)\rangle}J_z$ for $g=0.001$ (full black) $g=0.15$ (full light gray) $g=0.3$ (dotted gray). The parameter values are $J=6$; $\beta=0.025$; $\mu=0.5$.

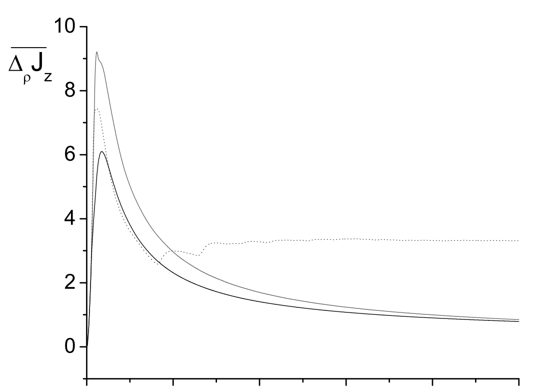

Fig. 7. Illustrated are time averages of the total dispersion $Tr[\rho(t)J_z]$ for $g=0.001$ (full black) $g=0.15$ (full light gray) $g=0.3$ (dotted gray). The parameter values are $J=6$; $\beta=0.025$; $\mu=0.5$.

analyzed. The environment is modeled by a dissipative nonlinear quantum oscillator in a macroscopic regime and the quantum system in interaction with this environment was represented by angular momentum variables $J_{x,y,z}$ with nonlinear Hamiltonian which preserved the size of the angular momentum $J_x^2+J_y^2+J_z^2$. The interaction between the system and the environment was taken to be linear in J_z and the coordinate Q of the macroscopic environment: $H_{int}=\mu J_z Q$. Our main interest was in the dependence of dynamics of the dispersion of the pointer observable J_z on the classically qualitatively different types of the environmental dynamics.

In order to be able to represent different types of dynamics and in particular the classically chaotic motion of the macroscopic environment we employed the quantum state diffusion description of an open quantum system dynamics. It is well known that in this description the evolution of $\langle\psi(t)|Q|\psi(t)\rangle$ and $\langle\psi(t)|P|\psi(t)\rangle$ during the stochastic process $|\psi(t)\rangle$ in the macroscopic limit resembles well the chaotic attractor of the classical Duffing oscillator for the appropriate parameter values. In fact, we used QSD approach to open system dynamics in several ways: (a) to represent classically chaotic or regular dynamics of the quantum but macroscopic nonlinear dissipative environment; (b) as the numerical tool to efficiently compute the dispersion in the system's mixed state $\rho(t)$; and (c) to gain further insight by analyzes of the dynamics of the dispersion in the random pure states $|\psi(t)\rangle$ that constitute the QSD unraveling of $\rho(t)=E[|\psi(t)\rangle\langle\psi(t)|]$.

Our numerical results clearly show that the total dispersion in the mixed state $\Delta_{\rho(t)}J_z=Tr[\rho(t)J_z^2]-Tr[\rho(t)J_z]^2$ approaches zero and remains very small all the time when the attractor of the environmental dynamics is regular, i.e. the stationary state or the limit cycle. On the other hand, $\Delta_{\rho(t)}J_z$ is significantly larger then zero when the environment has classically chaotic dynamics. Proper understanding of this result was made possible by studying the dynamics of the purely quantum dispersion in the random state $\Delta_{|\psi(t)\rangle}J_z=\langle\psi(t)|J_z^2|\psi(t)\rangle-\langle\psi(t)|J_z|\psi(t)\rangle^2$. In the cases of regular environmental dynamics this quantity quickly approaches and stays near zero for all the time. On the other hand, when the environment is classically chaotic $\Delta_{|\psi(t)\rangle}J_z$ quickly approaches zero but than experiences large variations away from zero, followed by quick convergence to zero and novel large variations. Large variations of $\Delta_{|\psi(t)\rangle}J_z$ occur simultaneously with large chaotic variations of the environmental variable $\langle Q(t)\rangle$. Averaging over the en-

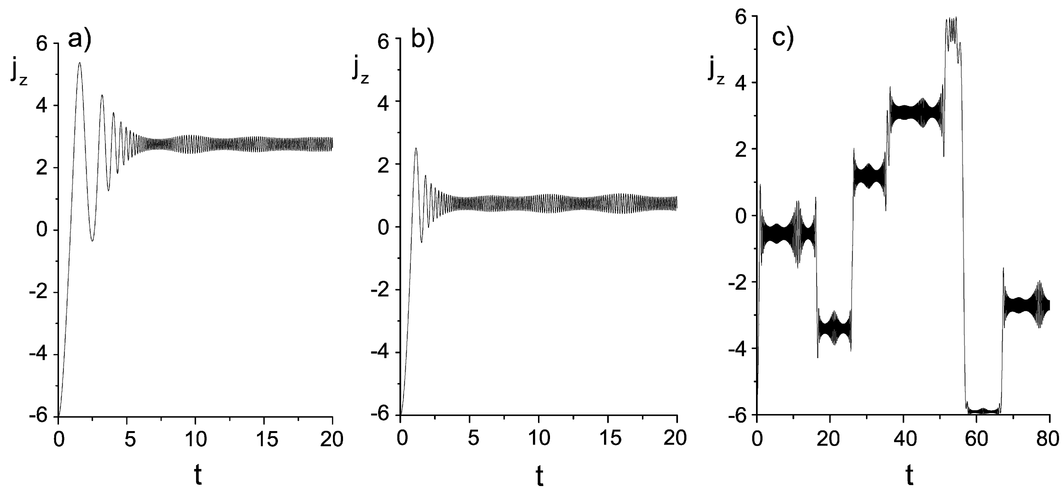

Fig. 8. Illustrates the evolution of the classical model. Presented are: $j_z \equiv \langle J_z \rangle$ for (a) $g = 0.001$; (b) $g = 0.15$ and (c) $g = 0.3$. The parameter values are $J = 6$; $\beta = 0.01$; $\mu = 0.5$.

semble of random pure states $|\psi(t)\rangle$ to obtain the mixed state $\rho(t)$ produces constantly large values of the total dispersion $\Delta_{\rho(t)} J_z$, and masks the dynamical origin of large dispersion values. It is important to stress that in the macroscopic limit treated here other types of unraveling of the master equation for $\rho(t)$ would produce similar quantum trajectories and similar dynamics of the quantum dispersion $\Delta_{|\psi(t)\rangle} J_z$. In this sense the dynamical explanation of the large dispersion of the pointer variable when the environment is classically chaotic is independent of the particular unraveling (in our case QSD approach) and thus represent a true property of the quantum system.

Dependence of $\langle J_z \rangle$ and its dispersion on the other parameters characterizing the system or the environment is as one would expect. Larger J implies faster approach to zero of the dispersion, but also larger variations of $\langle J_z \rangle$ in the case of the chaotic environment. We have not studied the role of the parameter c characterizing the nonlinearity of the system. In fact, the qualitative properties of the system's dynamics in the macroscopic limit, characterized by large values of J, can be altered by introducing a periodic dependence on time of the parameter α, which was set to constant value in our computations. In this way one would be able to study the interplay of the chaotic environment with complicated system's dynamics. The role of the magnitude of the coupling parameter is qualitatively clear. As far as the environment is considered the role of the bifurcation parameter g was the main theme of our work. The classicality parameter β was in our work always fixed to small values so that the environment behaved as a macroscopic system. In the case of $\beta = 1$, corresponding to the purely quantum environment, no qualitative difference was observed between the behavior of the pointer observable and other observables that do not commute with the interaction Hamiltonian.

In summary, our work shows that decoherence is faster with the chaotic macroscopic environment but such conclusion can be obtained and properly understood only if the macroscopic limit of a single quantum system instead of an ensemble of systems is analyzed.

Acknowledgements

This work is partly supported by the Serbian Ministry of Science contract No. 141003. I would also like to acknowledge the support of Abdus Salam ICTP.

References

[1] M. Schlosshauer, Decoherence and the Quantum-to-Classical Transition, Springer, Berlin, 2007.
[2] W.H. Zurek, Rev. Mod. Phys. 73 (2003) 715.
[3] E. Joss, H.D. Zeh, C. Kiefer, D. Giulini, J. Kupech, I.-O. Stamatescu, Decoherence and the Appearance of the Classical World in Quantum Theory, 2nd ed., Springer, New York, 2003.
[4] J.N. Bandyopatdyay, Quantum chaotic system as a model of decohering environment, arXiv:0806.4517v1 [quant-ph], 2008.
[5] J.W. Lee, et al., Phys. Rev. A 72 (2005) 012310.
[6] D. Rossini, G. Benenti, G. Casati, Phys. Rev. E 74 (2006) 036209.
[7] J. Lages, et al., Phys. Rev. E 72 (2005) 026225.
[8] S. Yuan, M.I. Katsnelson, H. de Raedt, Phys. Rev. B 77 (2008) 184301.
[9] A. Relaño, J. Dukelsky, R.A. Molina, Phys. Rev. E 76 (2007) 046223.
[10] R. Blume-Kohut, W.H. Zurek, Phys. Rev. A 68 (2003) 032104.
[11] L. Ermann, J.P. Paz, M. Saraceno, Phys. Rev. A 73 (2006) 012302.
[12] D. Cohen, T. Kottos, Phys. Rev. E 69 (2005) 055201(R).
[13] N. Buric, Phys. Rev. A 79 (2009) 022101.
[14] M.J. Everitt, W.J. Munro, T.P. Spiller, Quantum measurement with chaotic apparatus, arXiv:0905.1867v1 [quant-ph], 2009.
[15] I.C. Percival, Quantum State Diffusion, Cambridge Univ. Press, Cambridge, 1999.
[16] A.M. Perelomov, Generalized Coherent States and Their Applications, Springer-Verlag, Berlin, 1986.
[17] F. Trimborn, D. Witthaut, H.J. Korsch, Phys. Rev. A 77 (2008) 043631.
[18] T.A. Braun, I.C. Pecival, R. Schack, J. Phys. A: Math. Gen. 29 (1996) 2077.
[19] H.-P. Breuer, F. Petruccione, The Theory of Open Quantum Systems, Oxford Univ. Press, Oxford, 2001.
[20] V.P. Belavkin, Rep. Math. Phys. 43 (1999) 405.
[21] H.J. Carmichael, An Open Systems Approach to Quantum Optics, Springer-Verlag, Berlin, 1983.
[22] V. Gorini, A. Kossakowski, E.C.G. Sudarshan, J. Math. Phys. 17 (1976) 821.
[23] G. Lindblad, Commun. Math. Phys. 48 (1976) 119.
[24] J. Halliwell, A. Zoupas, Phys. Rev. D 52 (1995) 7294.
[25] L. Diósi, N. Gisin, J. Halliwell, I.C. Percival, Phys. Rev. Lett. 74 (1995) 203.
[26] W.T. Strunz, I.C. Percival, J. Phys. A 31 (1998) 1801.
[27] M.J. Everitt, New J. Phys. 11 (2009) 013014.
[28] M. Everitt, Phys. Rev. E 75 (2007) 036217.
[29] N. Buric, Phys. Rev. A 73 (2006) 052111.
[30] N. Buric, Ann. Phys. (NY) 323 (2008) 17.
[31] N. Buric, Phys. Rev. A 80 (2009) 014102.
[32] T.A. Brun, N. Gisin, P.F. O'Mahony, M. Rigo, Phys. Lett. A 229 (1997) 267.
[33] J. Guckenheimer, P. Holmes, Nonlinear Oscillations, Dynamical Systems and Bifurcations of Vector Fields, Springer-Verlag, New York, 1983.
[34] H.M. Wiseman, G. Milburn, Phys. Rev. A 47 (1992) 642.
[35] K. Molmer, Y. Castin, J. Dalibar, J. Opt. Soc. Am. B 10 (1993) 524.